

Emma Gleeman (Brown University, Providence, RI, USA)

Aaron Rachels (Brown University, Providence, RI, USA)

Andreas Schmittner (Oregon State University, Corvallis, OR, USA)

21 August 2015

What do Atlantic  $\delta^{13}\text{C}$  measurements indicate about AMOC shutdown and reinvigoration during the LGM–HS1 and HS1–Bølling-Allerød transitions?

### Abstract

$\delta^{13}\text{C}$  isotope records contain information about carbon storage in the ocean, air-sea gas exchange, and the functioning of circulation systems. It is currently believed that the Atlantic Meridional Overturning Circulation (AMOC) underwent dramatic changes in strength during the most recent deglacial period (20,000-10,000 aBP). Through its impact on the efficiency of the biological pump and vertical and horizontal transport, the variability of the AMOC is likely to be reflected in  $\delta^{13}\text{C}$  records. Geographically wide-ranging  $^{13}\text{C}$  data taken from benthic foraminifera in sediment cores were organized and compiled from different sources into a new comprehensive database. Here we discuss records from the Atlantic Ocean during the last deglacial period from this database. Millennial averages were calculated and spatially averaged into latitude and depth zones. Averages of isotope records were used to assess Atlantic circulation changes over the course of climate events: Last Glacial Maximum (LGM), Heinrich-Stadial 1, and the Bølling-Allerød. Decreasing trends in the early deglacial were found in the intermediate ocean in two of three latitudinal zones.  $\delta^{13}\text{C}$  averages stayed relatively constant in the late deglacial in intermediate ocean zones. A late-deglacial increase of about 0.3-0.5 per mille was found in the deep ocean in all three latitudinal zones, supporting previous studies of possible late-deglacial massive carbon release from the deep ocean.

### Introduction

This project analyzes a wide range of carbon isotope ratio observations from sediment cores located throughout the Atlantic Ocean to detect ocean circulation changes during the last deglaciation. Benthic  $\delta^{13}\text{C}$  records compiled into a new database lend insight into the changes in the AMOC from the late Last Glacial Maximum throughout

the climate events that followed: the Heinrich-Stadial 1 (18,000-15,000 aBP) and the Bølling-Allerød (15,000-13,500 aBP).

The purpose of this project is twofold; in addition to synthesizing time series of  $\delta^{13}C$  throughout the deglaciation to examine AMOC changes, we have produced a newly comprehensive and extensive database of most of the currently available published  $\delta^{13}C$  benthic data. Thousands of different data sets from different sites exist worldwide for benthic  $\delta^{13}C$  alone. Compilations of ocean sediment data that include benthic  $\delta^{13}C$  have been created previously (e.g. Oliver 2010), and modern, publicly-available databases such as NOAA contain abundant information. However, consolidating all existing  $\delta^{13}C$  data and maintaining one repository for new additions is a crucial step in ensuring that, for all paleoceanographic studies employing  $\delta^{13}C$  as a proxy, as full and updated a range of data as possible will be consistently available and that the data can be easily extracted and analyzed. A primary goal of this project has been to create this repository as a central starting point for a diverse group of scientists who are working to understand deglacial climate changes. Ocean Circulation and Carbon Cycling, or OC3, is an international collaboration through the Past Global Changes working group. It seeks to explore, through model simulations and the collection of data, the changes in ocean circulation and carbon storage on the glacial-interglacial timescale, and their controls on atmospheric  $CO_2$  levels. As it progresses, the OC3 project may improve our understanding of the roles that oceanic processes play in changing Earth's climate, and it could help to constrain and refine models that contribute to scientific knowledge of past and potential future oceanic and atmospheric conditions. The database produced as a result of this summer REU project may be the most complete and current collection of benthic  $\delta^{13}C$  information in the world. It will be continuously built upon and refined by the addition of newer datasets and improved age models. The database serves as an excellent foundation of carbon isotope information not only for the OC3 project, but also for other paleoceanography investigations in the future.

### Background

$\delta^{13}C = \frac{13C_{12C_{sample}}}{12C_{12C_{standard}}} - 1 \cdot 1000$  is a measure of the ratio of two stable carbon isotopes with respect to a standard. The global average  $\delta^{13}C$  of surface ocean water is 2‰. Photosynthesis by phytoplankton tends to fractionate at a ratio of ~-21‰

(Schmittner et al. 2013). When organic matter sinks down from the surface to the deep ocean and is respired, it contributes an isotopically light signal to the dissolved inorganic carbon, or DIC, of the deep ocean and leaves the surface ocean slightly enriched in  $^{13}\text{C}$ . Benthic foraminifera, single-cell organisms that live at the seafloor, incorporate the DIC signal of surrounding water into their carbonate shells with little fractionation, yielding an accurate paleo-record of deep-ocean carbon isotope ratios (Duplessy et al. 1984; Schmittner et al. 2013).

The last deglaciation saw considerable changes in atmospheric concentrations of greenhouse gases, namely an 80-ppm increase in  $\text{CO}_2$  (Marcott et al. 2014). Among various proposed explanations, the shutdown of the Atlantic Meridional Overturning Circulation, or AMOC, during the early deglacial Heinrich-Stadial 1 period has been discussed as a possible cause for abrupt changes in atmospheric temperature and  $\text{CO}_2$ . These sudden changes have been linked to the AMOC using Pa/Th data (McManus et al. 2004) and  $\delta^{13}\text{C}$  (Lund et al. 2015), as well as coupled ocean-biosphere-atmosphere modeling (Schmittner and Galbraith, 2008). The AMOC sends sinking waters in the North Atlantic southward at intermediate depths. This North Atlantic Deep Water rises back up to the surface near Antarctica and travels northward, becoming depleted in nutrients such as phosphate, and enriched in  $^{13}\text{C}$ , as it passes through highly productive zones in the tropics and subtropics.

Coupled ocean-atmosphere models are an important tool for investigating the relationship between AMOC shutdown, ecosystem responses, and atmospheric chemistry. Schmittner and Lund (2015) use  $\delta^{13}\text{C}$  data and model results to suggest that the early deglacial rise in atmospheric  $\text{CO}_2$  levels may have resulted from AMOC shutdown, which would have stopped the input of nutrient-depleted water to the mid-deep Atlantic Ocean. (The major uncertainty in the model results for LGM-HS1 published by Schmittner and Lund 2015 lies in the starting conditions for the model: preindustrial rather than glacial.) Without this input, the deep-water inputs to the Atlantic come solely from Antarctic Intermediate and Antarctic Bottom waters. These waters contain high levels of nutrients because they outcrop at, and source from, high Southern-Hemisphere latitudes where polar night inhibits photosynthetic production. With the Atlantic nutrient profile higher and no upward NADW motion at high Southern latitudes,

nutrients remain trapped at depth and nutrient deficiency at the surface inhibits phytoplankton productivity (Schmittner, 2005).

Schmittner and Lund's (2015, p.140) modeling results indicate that the ceased input of biologically light carbon to the deep oceans increases the  $\delta^{13}\text{C}$  of the deep ocean by 0.4‰ to 1.0‰ in the South and North Atlantic, respectively. The dampening of the biological pump causes outgassing of  $\text{CO}_2$  from the ocean to the atmosphere (Schmittner and Lund, 2015). These  $\delta^{13}\text{C}_{\text{DIC}}$  analyses using the MOBI 1.4 model show that, between years 0 and 2500 in their model, the North Atlantic becomes isotopically lighter and the South Atlantic heavier (p.142). This pattern agrees with a lack of preferential  $^{12}\text{C}$  uptake by surface biological processes, and lack of remineralization of light carbon that accumulates in the south from the AMOC and falling POC, respectively.

During the Bølling-Allerød, a period of warming that started 14.7 kyr ago, the AMOC restarted with a vengeance (McManus et al., 2004). Various theories seek to explain what triggered this reinvigoration. A transient model simulation, starting from LGM conditions and running until the Bølling-Allerød, triggered the AMOC restart as a response to the termination of freshwater input to the North Atlantic (Liu et al. 2009). This study reported that the recovery of the AMOC, coupled with the effects of increased atmospheric  $\text{CO}_2$ , caused the BA warming. Thiagajaran et al. (2014) used a variety of methods such as  $\delta^{13}\text{C}$ ,  $\delta^{14}\text{C}$ , and U/Th analyses to propose that the cause of the BA warming was a change in density structure originating in the deep ocean, which stayed relatively calm during HS1; a temperature inversion, stabilized by salt stratification, stored warm water of unknown origin at depth, creating a reservoir of heat energy that was suddenly released to the surface when deep waters "punched through" upper layers. Mignot et al. (2007) ran a coupled climate model to investigate the thermal profile of Atlantic waters during the shutdown and recovery of the AMOC, and also attribute the rapid reinvigoration to a temperature inversion in the water column. Lund et al.'s (2015) investigation of the evolution of the Southwest Atlantic during the last deglaciation, based on Brazil Margin cores, reports no drastic change in deep-sea benthic  $\delta^{13}\text{C}$  between 22 and 16 kyr BP. During this early deglacial period, which includes HS-1, intermediate Atlantic waters see a  $\delta^{13}\text{C}$  decrease of about 0.5‰, underscoring the temporal offset

between changes in intermediate ocean layers (earlier) and deep ocean layers (later) during the deglaciation.

### Methods

In order to build the database that was used for these analyses and that will serve as the foundation of benthic  $\delta^{13}\text{C}$  data for the OC3 project, we needed to choose a system that would both easily enable future contributions and make the database easily accessible. Our research team decided that formatting the database using Microsoft Excel would allow for maximum flexibility in these regards. The database includes a master spreadsheet as well as separate sheets for each individual site included in the database. One of the most salient features of the database is its ability to enable the updating of age models as new and improved age models are published. Therefore, the information on how each  $\delta^{13}\text{C}$  record was calibrated—for instance, radiocarbon tie points—is included in a site-specific age tab adjacent to that site's tab in the database.

A first important step entailed extracting applicable data from both of our two main sources: Olivier Cartapanis's database and Andreas Schmittner's collection of  $\delta^{13}\text{C}$  data files. We worked closely with Cartapanis to code the extraction of meaningful data ( $\delta^{13}\text{C}$ ,  $\delta^{18}\text{O}$ , depth, age, and various pieces of site-specific information such as latitude, longitude, site depth, species, author, and publication). For the Schmittner data collection, individual data files were evaluated and added to the OC3 database if they were found to contain the necessary data.  $\delta^{13}\text{C}$  and either depth or age information were the minimum criteria for addition to OC3. The other source of data from which we extracted the current contents of the OC3 database is the NOAA online database of core records; the Cartapanis database comprised all records from NOAA and Pangaea as of December 2011, so the more recent NOAA cores were added. Fig. 1 shows the geographic distribution of all data.

As previously mentioned, age models are an extremely important part of the OC3 database project. Many of the cores in the database do not have age information attached; many do have age models, but in order to render the OC3 database the best possible tool, it is desirable to align as many cores as possible along a common time scale, in the highest resolution possible, using a verified method. Over the course of this project, we have corresponded with Lorraine Lisiecki and Carly Peterson regarding the best way to

attach and correct age information. Please see Conclusions/ Future Work for more detailed description of the utility of Lisiecki's *Match* software in the next steps of this project. Age models for 114 cores in the OC3 database were updated with age models provided by Carlye Peterson and published in Stern and Lisiecki 2014.

In order to analyze only the data pertaining to my specific research question, I applied various filters to the OC3 master spreadsheet. I identified Atlantic sites by filtering for longitudes between -80 and 30, manually adding Atlantic sites not included in this data range (ie, several sites just north of South America's northeast coast). Given that I am conducting my investigation on the deglacial time period, I filtered by age to collect data points only between 20 ky bp and 10 ky bp. This time period does not capture the entire LGM, but it places the starting point of my period of study well within the LGM. I also filtered for resolution, making sure that for my data analysis I only extracted sites that feature millennial- or near-millennial-scale resolution.

Subsequently, I wanted to divide my data into latitudinal zones. To ensure that every zone would have a similar number of sites for a more consistent analysis, I examined the latitudinal distribution of sites and concluded that appropriate borders for South/ Equatorial and Equatorial/ North zones would be -16 degrees and 34 degrees, respectively. A similar strategy was employed to create Intermediate vs. Deep zones for site depth; Figure 3 shows that the distribution of depth sites trends toward deeper site depths at more southern latitude. Based on the goal of creating depth sections with roughly equivalent numbers of sites for each latitudinal zone, I chose different depth cutoffs for South, Equatorial, and North: -3500 m, -3000 m, and -2000 m, respectively.

To facilitate the search for trends in  $\delta^{13}C$ , I created averages of  $\delta^{13}C$  for each of the ten millennia encompassed in the time period of my analysis for every core using the program R (see code in Supplementary Materials folder). The resulting millennial averages for each core were then spatially averaged within each latitude/depth zone. The time series of these millennial/ spatial averages can be found in figures 5, 6, and 7. Simple linear regression analysis was conducted for each millennium in each zone to assess the feasibility of using an average as an assessment of trend; additionally, analyses of the standard deviation of millennial  $\delta^{13}C$  change in each core in every region, as well as standard deviation of entire deglacial  $\delta^{13}C$  change in one region's cores, were

performed. The results of the regression analysis and the standard deviations of whole-deglacial changes can be found accompanying time series for each zone in the Results section.

To facilitate analysis of basin-scale change across each of the three time periods in question—LGM, HS1, and BA—cross-sectional contour plots along longitude were created in Matlab for each time period. A function in R, similar to that which was used to create millennial averages, was used to average each site's  $\delta^{13}\text{C}$  values within the time periods 20,000-18,000 aBP (LGM), 18,000-15,000 aBP (HS1), and 15,000-13,500 aBP (BA). These contour plots interpolate between the data points, serving as snapshots of the state of  $\delta^{13}\text{C}$  distribution in the Atlantic. Plots of the differences in these periods'  $\delta^{13}\text{C}$  values were also produced using these averages. (See Figure 9).

## Results

Following the compilation of the OC3 database, which currently contains some 491 sites, the filtering of the database to fit my criteria yielded a collection of 108 Atlantic sites for analysis. Figure 1 shows that these sites are largely concentrated in the East Atlantic and at mid- to high-latitude.

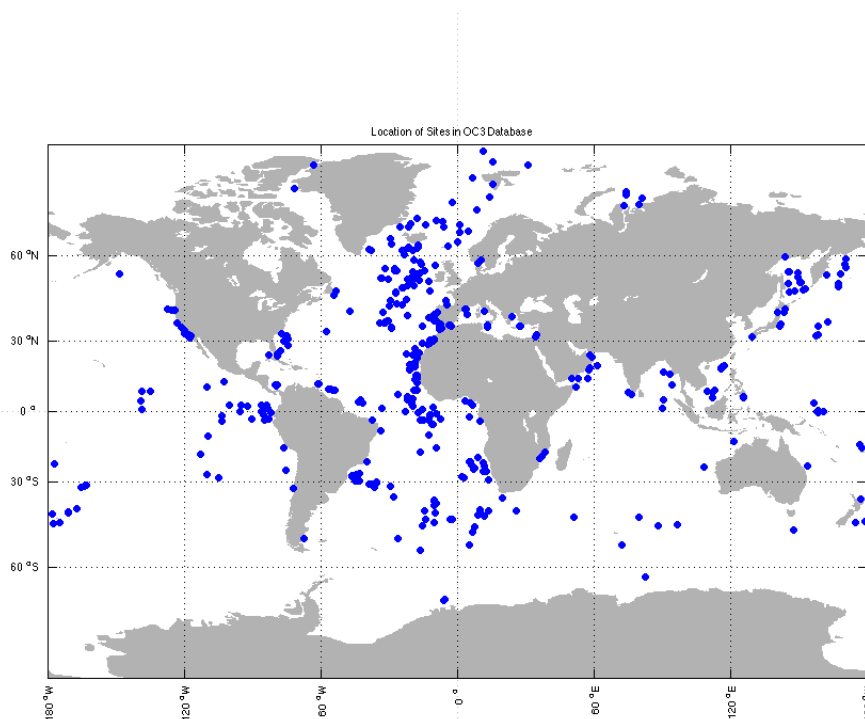
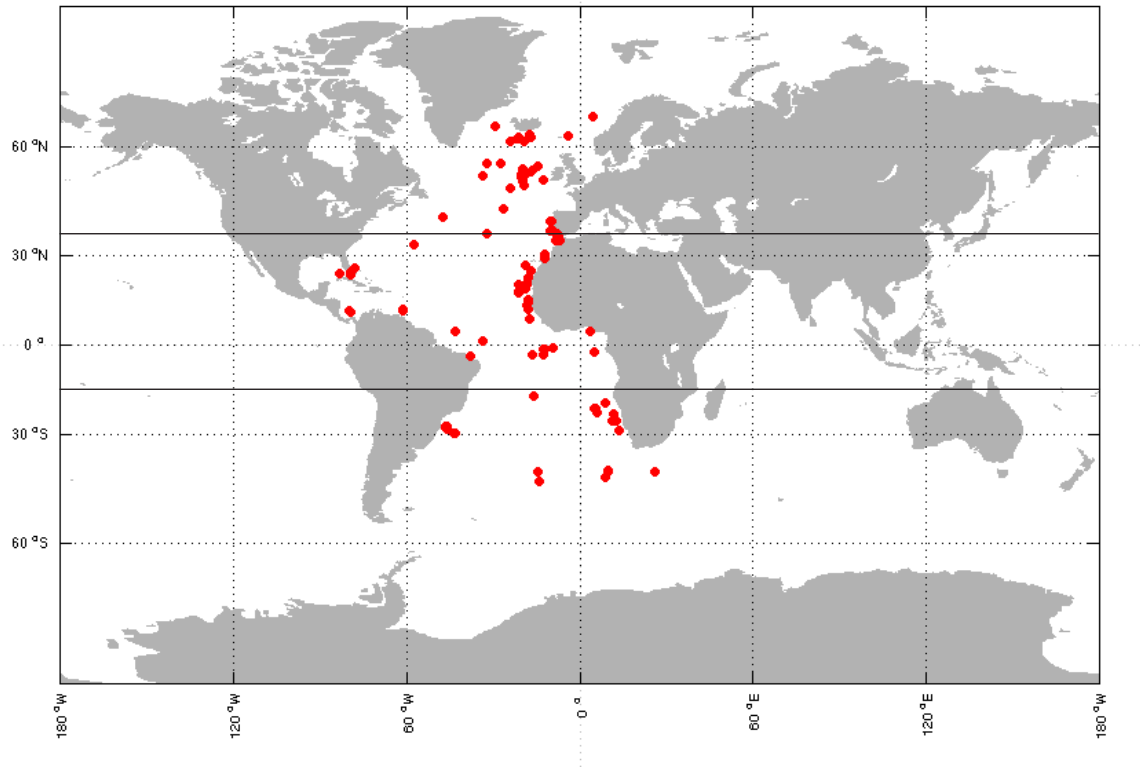


Figure 1.  
Map of all sites currently included in OC3 Database.

Figure 2. Map of OC3 Atlantic Sites used in this analysis



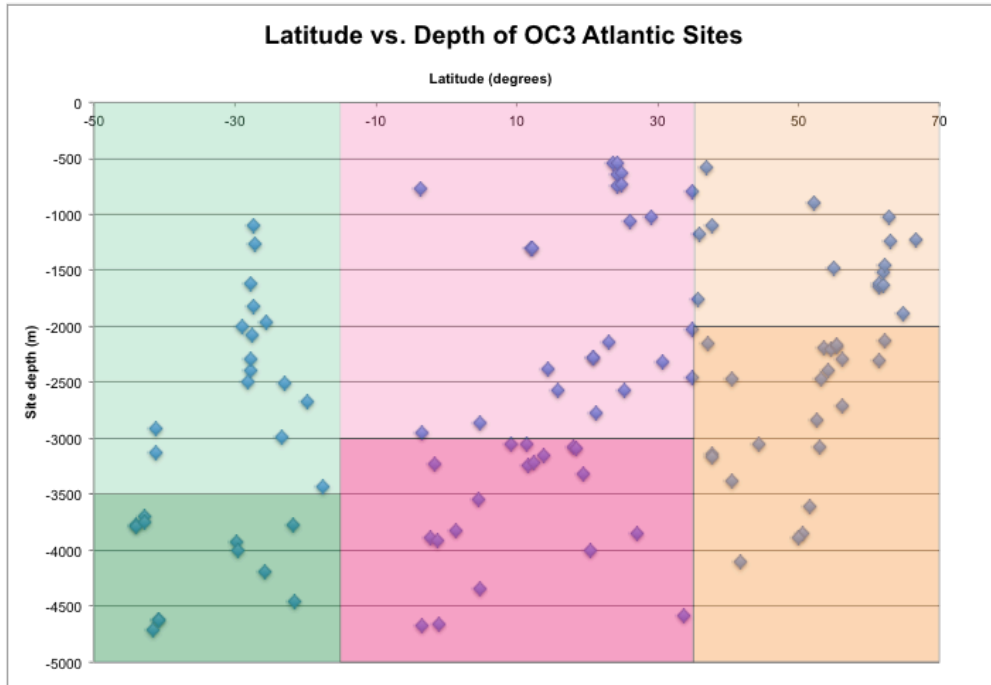


Figure 3. Latitude and depth distribution of Atlantic sites from OC3 database.

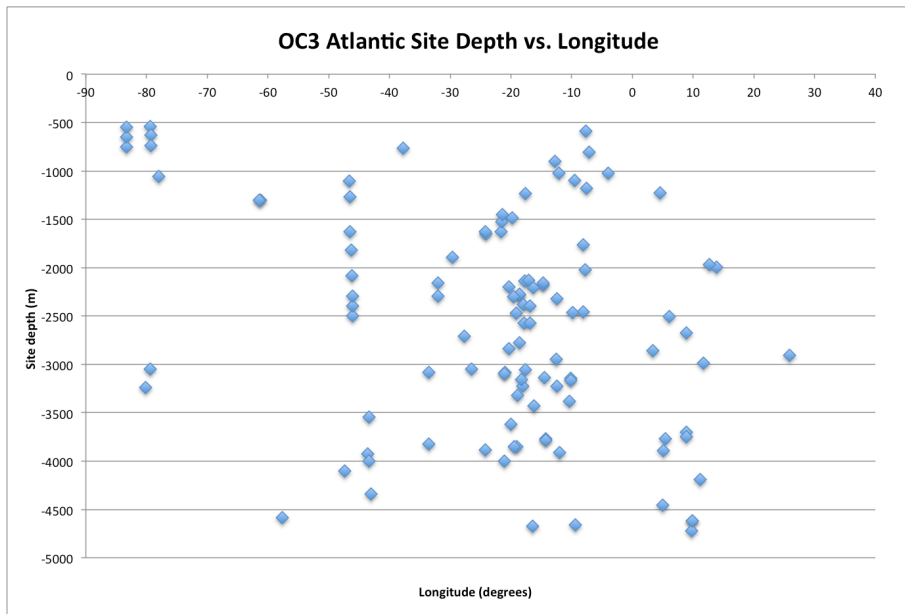


Figure 4. Longitudinal and depth distribution of Atlantic sites from OC3 database.

The plot of longitude vs. density, shown above, lends visual aid to the question of which areas, from east to west, are well-sampled and not-well-sampled. Several transects are visible, such as at about -47 degrees. In general, the East Atlantic is much more thoroughly sampled than the West Atlantic. The northwestern coast of Africa is especially well sampled, as reflected in the density of points around -20 degrees. There is a large gap in sites between -50 and -70 degrees. In the database, a multitude of sites with such locations exist; however, they did not feature a high enough resolution, or frequently did not contain records from the right time period, to be included in this study. Naturally, the depth distribution of this collection of sample sites is constrained by the bathymetry of the Atlantic.

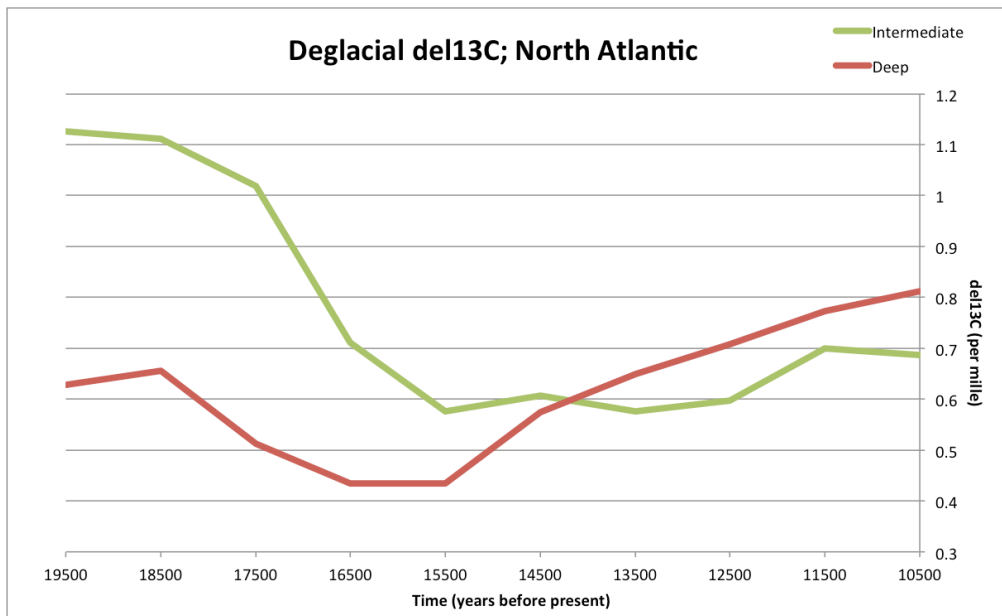


Figure 5. Time series of average d13C values for the North Atlantic. Below: table of millennial regressions and R<sup>2</sup> values for Deep Equatorial time series. Bottom: similar table for Intermediate Equatorial.

Age	Slope	R_Squared
10500	-0.000306442	0.108876052
11500	3.72E-05	0.002530671
12500	-0.000494845	0.213923076
13500	0.00043631	0.074791769
14500	-0.000226376	0.029077062
15500	0.000100653	0.009885792
16500	0.000273473	0.045276088
17500	0.000196817	0.033083412
18500	-2.23E-05	0.000477805
19500	-0.00019609	0.027656277
Age	Slope	R_Squared
10500	-4.46E-05	0.000236887

11500	0.000300323	0.011680981
12500	-0.000272992	0.006496353
13500	0.000108603	0.001198129
14500	0.000630408	0.05354631
15500	-0.000275933	0.015427865
16500	0.000217015	0.007042416
17500	0.000319068	0.014602802
18500	0.000108759	0.001267475
19500	0.000351331	0.017593347

Fig. 5 shows that in the millennial/ spatial average results for the North Atlantic, the deep ocean shows a slight increase in  $\delta_{13}C$  during the late LGM, then begins to decrease around 18,500 aBP, changing by approximately 0.2 per mille between 19,000 ky bp and 16,000 ky bp, a duration that mostly falls during Heinrich-Stadial 1. Around the beginning of the Bølling-Allerød, the deep North Atlantic starts to increase in  $\delta_{13}C$ , and reaches an increase of about .35 per mille by the end of the deglacial.

The intermediate North Atlantic decreases dramatically in the mid-deglacial, dropping by about .5 per mille from 20,000 to 15,000 aBP. The intermediate North Atlantic does not show a large increase toward the end of the deglacial;  $\delta_{13}C$  increases by only about 0.1 per mille beginning during the Younger Dryas.

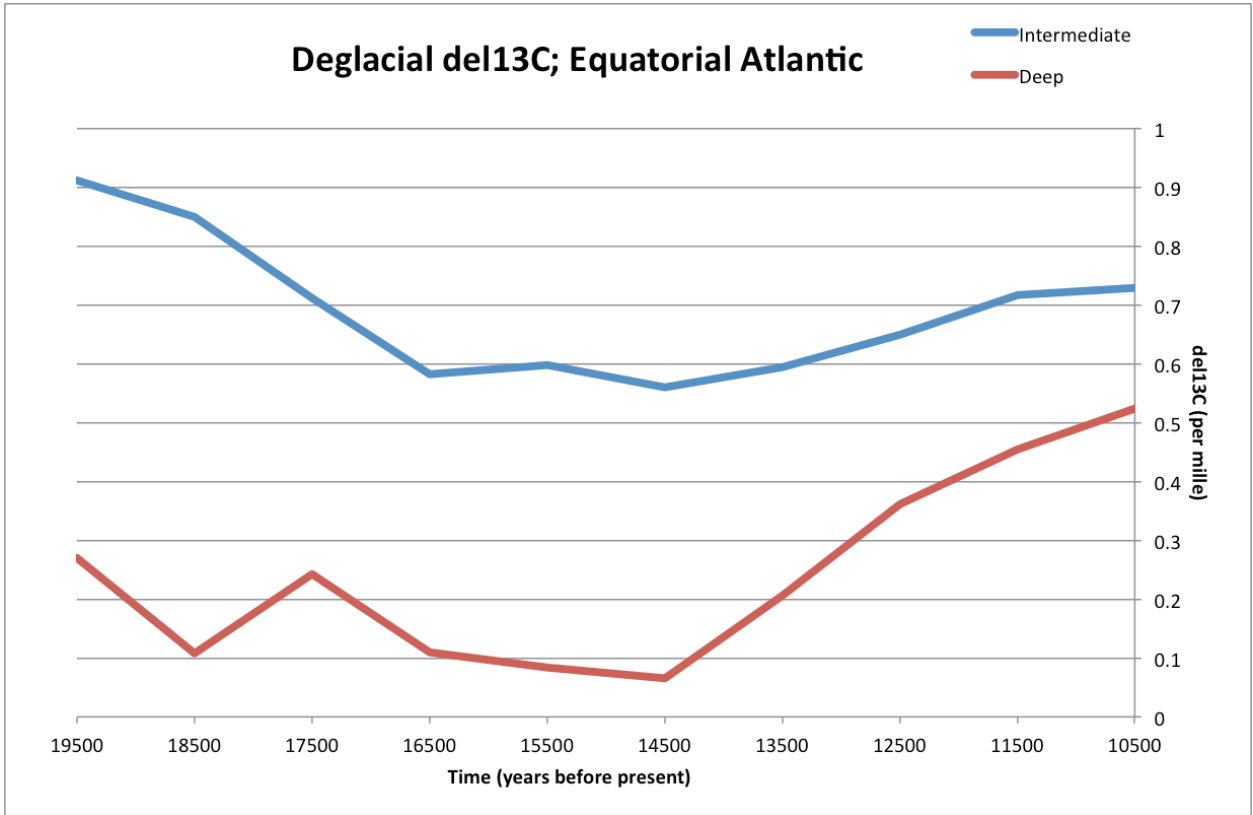


Figure 6. Time series of average  $\delta^{13}C$  values for the Equatorial Atlantic. Below: table of millennial regressions and  $R^2$  values for Deep Equatorial time series. Bottom: similar table for Intermediate Equatorial.

Age	Slope	R_Squared
10500	-0.000457735	0.132314412
11500	0.000138629	0.01222273
12500	-0.000444457	0.139971743
13500	-0.000328727	0.051916846
14500	-3.38E-05	0.000498381
15500	0.000231345	0.030253383
16500	-1.04E-05	0.000152182
17500	0.000193019	0.00500026
18500	4.29E-05	0.000794769
19500	0.000389934	0.013293532

Age	Slope	R_Squared
10500	4.28E-05	0.000914342
11500	0.00014689	0.007989323
12500	-0.000229036	0.023477344
13500	-5.77E-05	0.001037521
14500	0.00016741	0.012581637
15500	0.000138708	0.009245475
16500	0.000218355	0.012125009
17500	-0.000182279	0.008261713
18500	0.0003548	0.053564052
19500	-0.000211727	0.020897213

In the deep Equatorial Atlantic,  $\delta^{13}C$  does not change much until year 14,500 (Fig. 6). Subsequently, the deep  $\delta^{13}C$  increases dramatically around 14,500 aBP, attaining a change of about .45 per mille by the end of the deglacial.

In the intermediate equatorial Atlantic,  $\delta^{13}C$  decreases by about 0.25 per mille during HS1. There is only a slight increase of less than .05 per mille during the Bølling-Allerød.

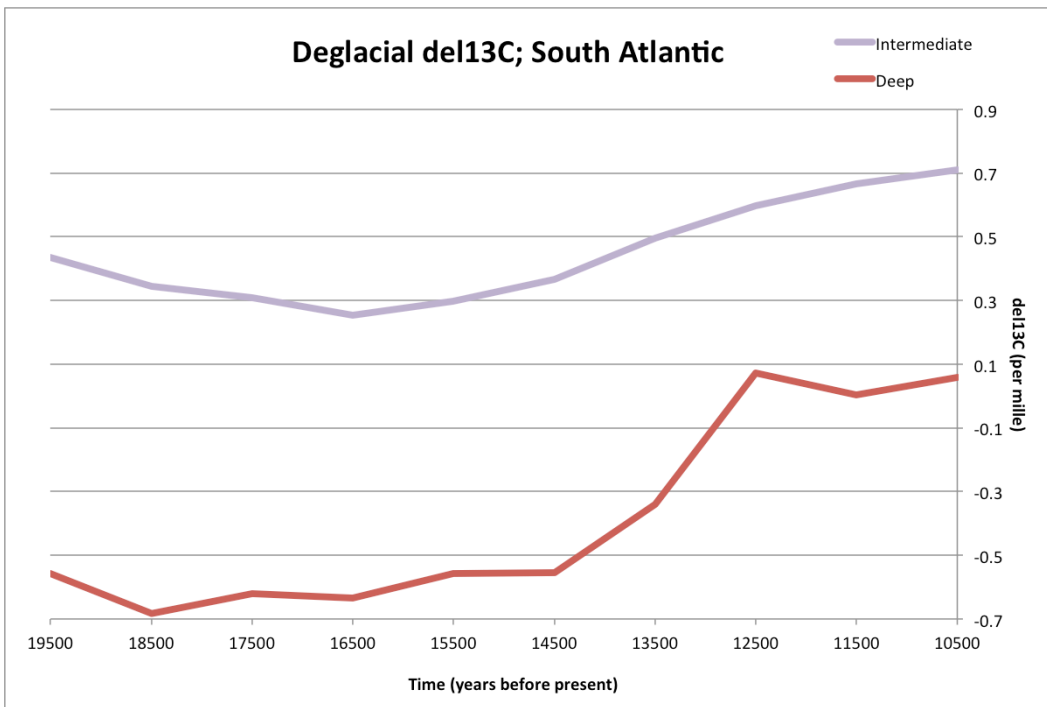


Figure 7. Time series of average  $\delta^{13}C$  values for the South Atlantic. Below: table of millennial regressions and  $R^2$  values for Deep South time series. Bottom: similar table for Intermediate South.

Age	Slope	R_Squared
10500	0.000421714	0.102212487
11500	0.000148867	0.020972554
12500	0.000303583	0.099082246
13500	-3.20E-06	3.77E-06
14500	0.000270545	0.039439986
15500	0.000259339	0.041323214
16500	0.000290509	0.062591545
17500	0.000173438	0.020942902
18500	0.000110187	0.007613928
19500	2.42E-05	0.000109834

Age	Slope	R_Squared
10500	-5.55E-05	0.003774464
11500	-0.00026106	0.095501385
12500	-8.07E-05	0.006711024
13500	-3.15E-05	0.000594121
14500	-1.84E-05	0.000251618
15500	0.00016851	0.023739508
16500	-4.84E-06	2.09E-05
17500	0.000360242	0.075511295
18500	-6.31E-07	1.94E-07
19500	0.000212434	0.021113417

At southern latitudes, the intermediate Atlantic waters see only a very slight decrease of about 0.15 per mille between the LGM and the middle of HS1, beginning to climb again around 16,500 aBP and completing an increase of just over 0.2 per mille by the end of the Bølling-Allerød. However, because of the way the deep vs. intermediate zones are defined to include similar data densities in all boxes, the “intermediate” box here begins at greater depth than it does in the North and Equatorial Atlantic, including deep water above 3,500 m (Fig 3). The starting value of  $\delta^{13}C$  in the Southern Atlantic Ocean is notably lower than in the deep waters at more equatorial and northern latitudes, likely due to the older age and therefore greater quantity of accumulated respired light carbon. The deep South Atlantic stays relatively flat during the end of the LGM and the entirety of HS1, beginning to increase sharply during the Bølling-Allerød, about 14,500 years ago.

Figure 8. Whole-Deglacial  $\delta^{13}C$  change, beginning to end, and standard deviation of whole-deglacial change in individual cores in every region. Average millennial changes and standard deviations of cores’ millennial changes can be found in Supplementary Materials folder.

Region	Mean Overall Deglacial $\delta^{13}C$ Change	Std. Deviation of Whole Deglacial $\delta^{13}C$ Change
IN	0.459440766	0.480707244
DN	-0.180128712	0.318499989
IE	0.182507152	0.359313464
DE	-0.304341049	0.652546712
IS	-0.274849521	0.288740311
DS	-0.593616342	0.623179239

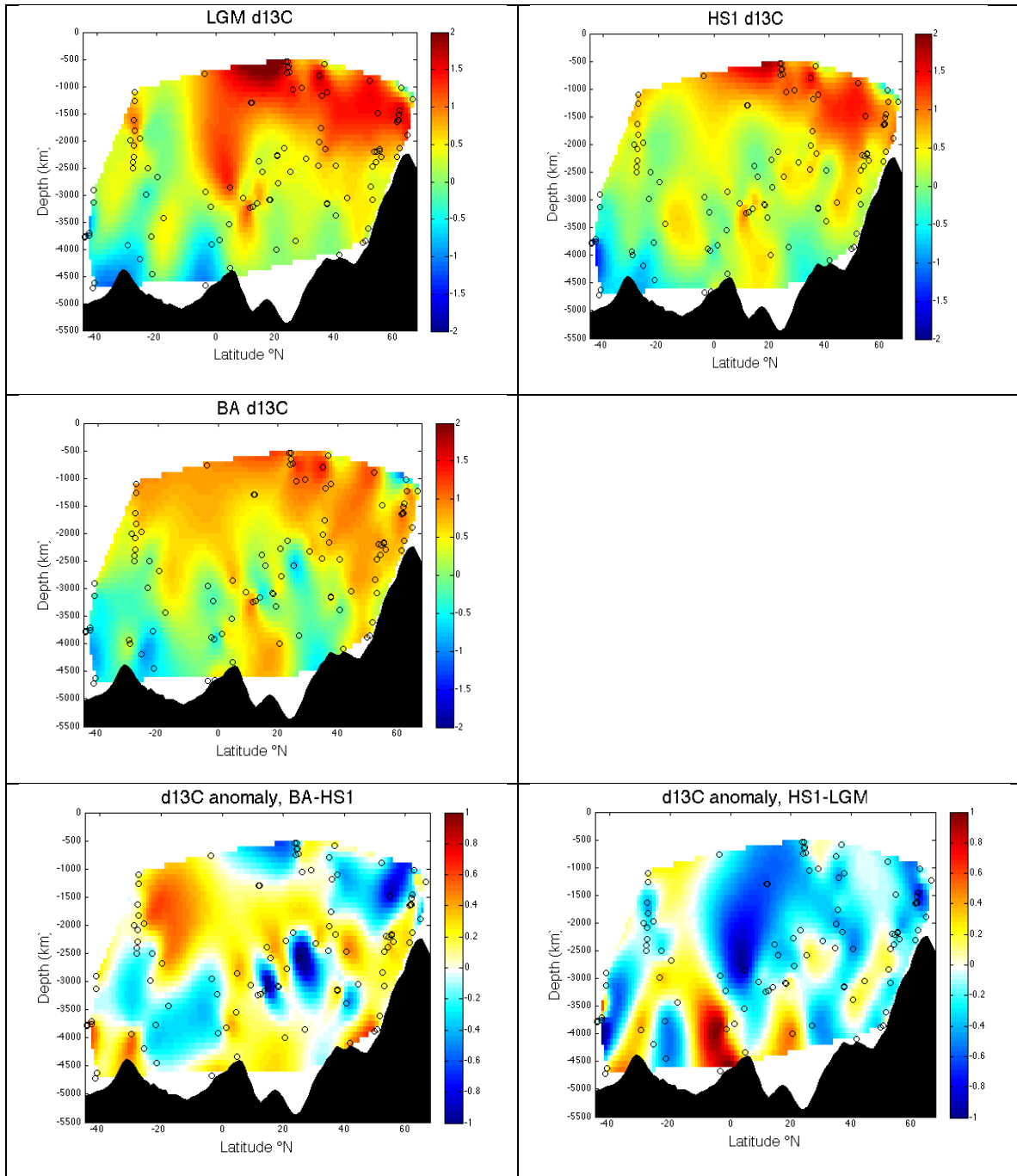


Figure 9. Longitudinal cross-section contour plots of  $\delta^{13}C$  values. Top left: Last Glacial Maximum, 20-18 ky bp. Top right: Heinrich-Stadial 1. Middle: Bølling-Allerød. Bottom right: Difference plot of Heinrich Stadial 1- Last Glacial Maximum. Bottom left: Difference plot of Bølling-Allerød – Heinrich Stadial 1.

These contour plots show the state of Atlantic  $\delta^{13}C$  collapsed longitudinally for three time periods: Last Glacial Maximum, Heinrich-Stadial 1, and Bølling-Allerød. The

fourth and fifth plots show the difference between  $\delta^{13}\text{C}$  values in the time periods HS1- LGM, and BA- HS1. Between LGM and HS1, there is an increase of up to 0.6 per mille at 4000 m depth just south of the Equator; this dramatic increase seems to be the interpolation result created by only one or two cores, which does not have the best age resolution, so it should not be considered as a real feature. There is a mild increase of 0.2 to 0.3 per mille throughout much of the rest of the deep ocean in all latitudinal zones. This difference plot also portrays a decrease throughout much of the intermediate ocean consistent with Figs. 5-7.

The contour plot of the difference between  $\delta^{13}\text{C}$  values in the Bølling-Allerød period and Heinrich-Stadial 1 shows an increase of about 0.2 to 0.5 in intermediate-ocean  $\delta^{13}\text{C}$ , especially toward southern latitudes. The plot also shows several spots of increase of about 0.2 to 0.3 in the deep ocean.

### Discussion

#### **North Atlantic**

The increase of 0.5 per mille in intermediate (0- 2000 m) North Atlantic  $\delta^{13}\text{C}$  (Figs. 5,9) is consistent with the picture of AMOC slowdown; during a normal AMOC period, surface waters in which biological processes deplete light carbon and leave the  $\delta^{13}\text{C}$  of DIC heavy. These heavy waters would sink to intermediate depths at northern latitudes. Without this input of heavy North Atlantic surface water, DIC drops dramatically. These results are consistent with the drop in observed  $\delta^{13}\text{C}$  in the North Atlantic as put forth in Schmittner and Lund (2015; see Appendix Fig. A2); the decrease that they describe has the largest magnitude at intermediate depths. However, the decrease in their model is larger than that in the sediment data. Surprisingly, the  $\delta^{13}\text{C}$  in the Intermediate North Atlantic stays relatively flat during the Bølling-Allerød, when an increase would be expected based on the theory of “Super-AMOC” reinvigoration. This is consistent with a recent examination of high-resolution  $\delta^{13}\text{C}$  data from the intermediate-depth North Atlantic by Oppo et al. (2015, Fig. A7), who find rather small and gradual changes from HS1 into the BA.

In the deep North Atlantic, there is a decrease in  $\delta^{13}\text{C}$  during the early deglacial period (Fig. 5,9). This decrease of magnitude 0.2 per mille is consistent with Schmittner and Lund’s (2015) results of a synthesis of  $\delta^{13}\text{C}$  observations; they reported a 0.2 per

mille decrease in  $\delta^{13}C$  at -3000 m in the North Atlantic from the LGM to the Heinrich-Stadial.

The dramatic increase in deep North Atlantic  $\delta^{13}C$  in the later deglacial aligns well with the theory of massive carbon release from the deep ocean, because lighter carbon would be preferentially released if the deep ocean were to suddenly purge its reservoir of biologically-sequestered carbon.

### **Intermediate Atlantic**

The intermediate (0- 3,000 m) Equatorial Atlantic lightening in  $\delta^{13}C$  in the early deglacial (Fig. 6) is consistent with reduced southward advection of light  $\delta^{13}C$  from the North Atlantic in case of an AMOC reduction. The subsequent increase in intermediate  $\delta^{13}C$  during the late deglaciation is very slight ( $\sim 0.2$  per mille), but possibly consistent with a reinvigorated AMOC once again depleting the mid-depth ocean depths of light carbon. This low-amplitude change is also consistent with modeling results from Schmittner and Lund 2015 (Fig. A2).

Though the increase in deep Equatorial Atlantic  $\delta^{13}C$  around 19,000 aBP could point to AMOC shutdown, it is more likely noise in the data because it is a fairly small increase and happens over a very short period of time before decreasing again during the next millennium. The deep Equatorial Atlantic is one of the regions that features the largest standard deviation in  $\delta^{13}C$  trends in each of its millennia; in particular, the standard deviations of its millennial changes between 19,500 and 18,500 is 0.524, compared to an average millennial change of 0.245 per mille. The average change during this millennium, however, is relatively large as compared to the rest of the deglacial; a relatively large average change and a large standard deviation in change might indicate that several cores' millennial change value is very large, while other cores changed very little during that millennium.

A dramatic increase in  $\delta^{13}C$  beginning around 14,500 years is possibly indicative of release of carbon from the deep ocean. However, the mechanism for carbon release from the deep ocean during the Bølling-Allerød is still not well understood.

### **South Atlantic**

In the Intermediate (0- 3,500 m) South Atlantic, the small decrease in  $\delta^{13}C$  during HS1 is possibly reflective of an AMOC shutdown and less biological uptake of

light carbon. Thus, the 0.2 per mille increase in intermediate  $\delta^{13}\text{C}$  between HS1 and the Bolling Allerod could indicate a restart of biological pump efficiency. However, both these changes are very slight.

The lack of notable change in the deep South Atlantic's  $\delta^{13}\text{C}$  during HS1 may be a surprising result. Schmittner and Lund note in their 2015 article that observed  $\delta^{13}\text{C}$  DIC decreases during the Heinrich-Stadial are less dramatic at southern latitudes and in deeper water than in more Northern cores and in the intermediate ocean. Inaccurate age models could possibly jumble the  $\delta^{13}\text{C}$  signal there. Another possibility is that the AMOC runs more deeply in modern times than during the deglacial (Schmittner and Lund 2015); in this case, the deep ocean would not necessarily pick up a signal from an AMOC shutdown in its  $\delta^{13}\text{C}$ .

The dramatic increase in  $\delta^{13}\text{C}$  in the deep water during the Bolling Allerod / Younger Dryas supports the theory of carbon release from the deep ocean during this period, echoing Lund et al. 2015's result of though, as previously mentioned, possible mechanisms for this release are still being put forth.

When considering the surprising lack of  $\delta^{13}\text{C}$  increase in the intermediate waters during the supposedly dramatic AMOC reinvigoration, one possible explanation is an offset in  $\delta^{13}\text{C}$  created by the isotopic composition of atmospheric  $\text{CO}_2$  during this time. Schmitt et al. 2012 found that, by the beginning of the Bølling-Allerød,  $\delta^{13}\text{C}$  of atmospheric  $\text{CO}_2$  was 0.3 per mille less than during the LGM (see curve B in Appendix 4). This decrease is interpreted to be the result of the degassing of isotopically light carbon from the ocean when biological pump efficiency dropped. A renewed advection of waters would allow this atmospheric signal to be transmitted into the ocean, offsetting a heavier composition of intermediate-depth Atlantic seawater. During the later parts of the deglaciation (B/A, Y-D), release of isotopically light carbon from the South Atlantic and mixing of this water with upper ocean waters in the return route of the AMOC could also have contributed to a relatively muted signal in the North Atlantic.

Though the contour plots of  $\delta^{13}\text{C}$  values during the three time periods do contain some puzzlingly stark color differences, several of the more widespread changes across periods do express themselves the way we would expect based on the shutdown/restart/ deep carbon release theories of the deglacial AMOC behavior.

The  $\delta^{13}\text{C}$  distribution during the LGM (Figure 9) aligns fairly well in the Deep South Atlantic and Intermediate North Atlantic with values in a similar plot of Atlantic LGM  $\delta^{13}\text{C}$  produced by Lynch-Stieglitz et al (Appendix 5); additionally, the picture of intermediate-ocean  $\delta^{13}\text{C}$  decrease between the LGM and HS1 echoes Schmittner and Lund's 2015 modeling results (see the lighter composition of  $\delta^{13}\text{C}$  in the bottom panel of Appendix 2). The increase in the deep ocean  $\delta^{13}\text{C}$  between the Last Glacial Maximum and Heinrich-Stadial 1, as portrayed in Figure 9, is expected based on decreased biological pump efficiency. Figure 9 demonstrates that one point around the bathymetric high likely interrupts the trend of  $\sim 0.2$  per mille deep ocean increase along much of the equatorial and North Atlantic deep ocean. A challenge of working with an interpolation function is that one point with a drastically different value than its surroundings will have a great visual effect on the color contours. The decrease in  $\delta^{13}\text{C}$  throughout much of the intermediate ocean is an expected result of an AMOC reduction, though the decrease seems unusually concentrated at a deep mid-latitude site, possibly a result of a poor age model.

The second contour plot of differences—figure 9, bottom left—shows an intermediate South Atlantic increase in  $\delta^{13}\text{C}$  that is consistent with a restart of the AMOC and with light carbon being replaced with heavier carbon at intermediate-depth waters by re-invigorated southward flow of NADW. Though the difference map is noisy, the sites in the Intermediate South Atlantic have very good age control—sub-centennial-scale resolution—indicating that this increase should not be dismissed as merely a feature created by interpolation. The deep-ocean increase reflects the possibility of release of light carbon from greater depths. I suspect that the blue spots of decrease found between areas of increase both at shallower and greater depths likely resulted from the difficulties of longitudinally collapsing the data.

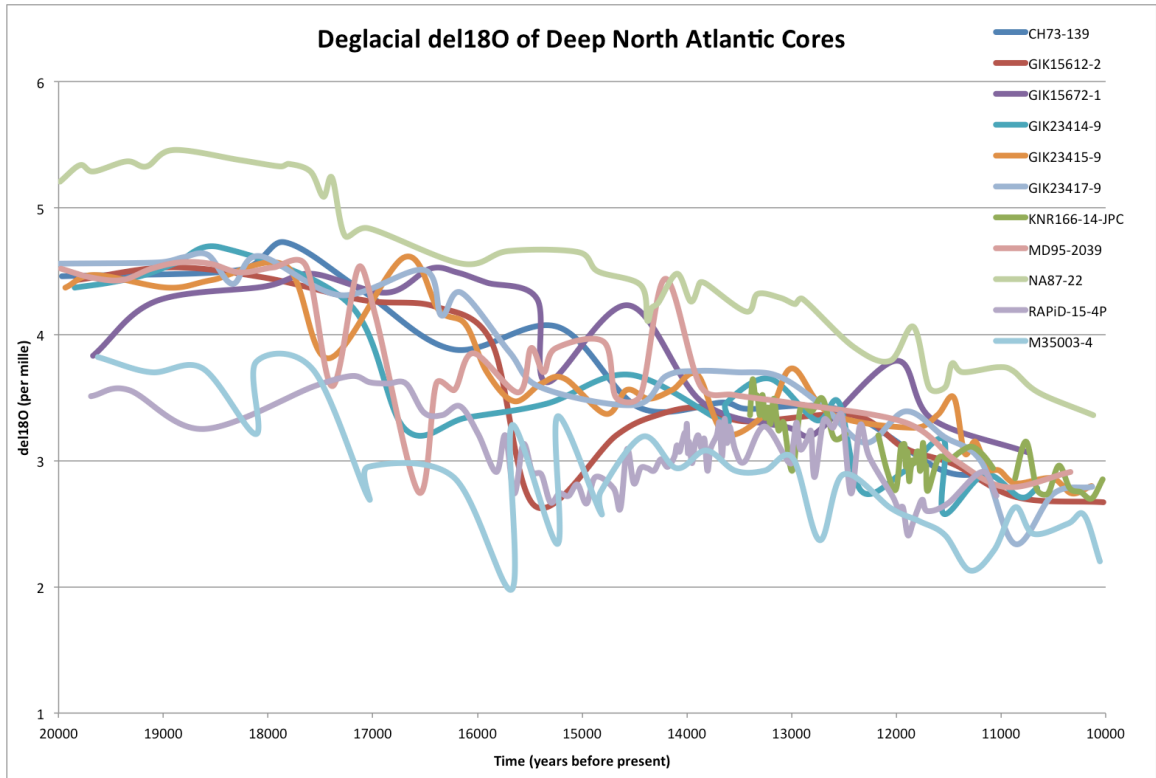


Figure 10. Collection of del18O curves from OC3 cores in the Deep North Atlantic. Note the great differences in resolutions and the different timings of early-mid-deglacial downward spikes, despite the general gentle downward trend in most cores. Several of these cores demonstrate a similar pattern of repeated high del18O values, such as NA87-22 and GIK15672-1, but with different durations and timing.

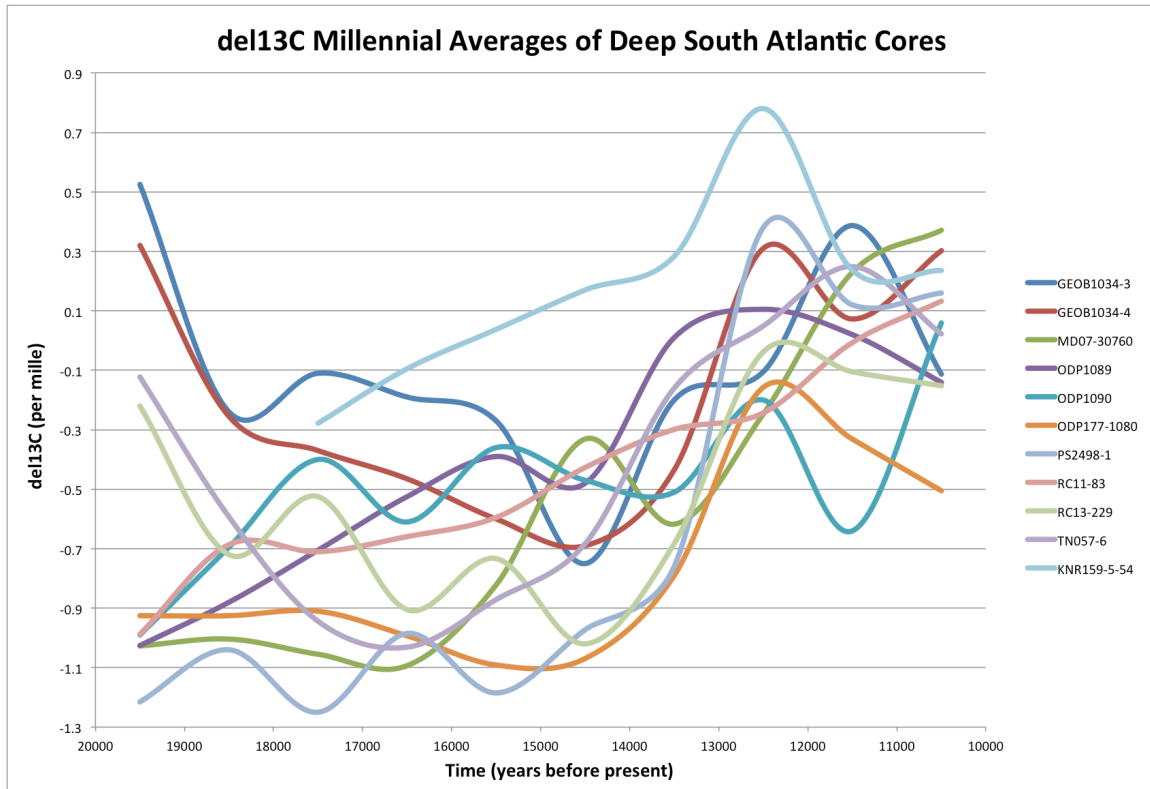


Figure 11. Example of Deep South Atlantic individual cores'  $\delta^{13}\text{C}$  values, averaged within each millennium. Note the overall flat to slight decreasing pattern of many cores in the very early deglacial and the sharp rise in  $\delta^{13}\text{C}$  in most cores toward the late deglacial. Overall, however, the collection is very noisy, with many disparate trends in different cores over shorter time periods within the deglacial. very noisy.

Overall, many problems arise with spatially averaging so many cores from disparate locations. Inevitably, these cores will have strongly varying  $\delta^{13}\text{C}$  values and also, possibly, age models that do not match. See Figure 10 for an example of  $\delta^{13}\text{C}$  values from different cores in the same latitudinal/ depth zone, and Figure 11 for an example of the great variability of these cores'  $\delta^{18}\text{O}$ , which can serve as a method of dating cores. As age models in the OC3 database are added, improved, and updated, regionally averaging cores will likely produce less deviation between individual cores' trends and spatial averages' trends, and will be a more feasible and accurate method for evaluating basin-scale oceanic changes. Plans for further work on OC3 database age models are elucidated in the Conclusion section.

## Conclusions

This investigation, in conjunction with my partner's investigation, is the first time that the brand-new OC3 database has been put into use in its intended fashion: filtered to provide the largest possible quantity of benthic  $\delta^{13}\text{C}$  data for a paleoceanographic investigation. This endeavor and its results are an exciting first step in analyzing  $\delta^{13}\text{C}$  to observe basin-wide trends using observation from highly spatially diverse sites.

Many expected changes in  $\delta^{13}\text{C}$  based on current knowledge are observed in the Atlantic Ocean, such as a sharp decrease in intermediate North Atlantic and intermediate Equatorial Atlantic  $\delta^{13}\text{C}$  in the early deglacial. The constancy of deep-water  $\delta^{13}\text{C}$  in the Equatorial and South Atlantic during the early deglacial indicates that the AMOC changes during that time affected only ocean layers above 3,000- 3,500 meters depth. It is likely that early deglacial analysis of the South Atlantic, the zone of study with the fewest datasets in this study, is hindered by the lack of data density and therefore the results are noisier and less reliable, perhaps with several cores canceling each other out. Another puzzling result is that lack of Intermediate North Atlantic increase in the late deglacial, since AMOC resumption at the onset of the B/A would be expected to produce a large increase there. However, decreasing atmospheric  $\delta^{13}\text{C}$  and release of isotopically light carbon from the South Atlantic, and mixing of this water with northward-flowing upper-Atlantic waters may partially cancel the effect of the AMOC resumption. As expanded upon below, future work conducting analysis of basin-wide Atlantic circulation change should seek to verify and improve age models. Right now, standard deviations of changes both across the whole deglacial and individual millennia are large compared to the average changes themselves, and  $R^2$  values of linear regression analyses are very small, indicating that it is difficult to fit one line to individual cores' trends and have it be a faithful average representation of change. Age model improvement in the OC3 database, as detailed below, should ameliorate this issue.

The late deglacial period shows clear, sharp increases in deep water  $\delta^{13}\text{C}$ , a result that echoes the Lund et al. 2015 result of a 0.5 per mille  $\delta^{13}\text{C}$  increase in the deep ocean after the Heinrich-Stadial period, though with lower magnitude; most Bølling-Allerød increases found in these analyses were about 0.2 or 0.3 per mille as opposed to the Lund result of 0.5 per mille. This late-deglacial increase is consistent across all three latitudinal zones.

This creation of the database and analysis of Atlantic data have been informative processes in that they have pointed to areas for continued work. Now that the OC3 database has been constructed and will serve as the main data vault for the OC3 project, there remains much room for improvement and expansion of the OC3 database. Firstly, the continual addition of data will render the database even more broadly useful and improve the spatial resolution of analyses such as this. Several data collections that were previously identified as target sources were unable to be mined for data within the time frame of this project. Alan Mix's collection of unpublished  $\delta^{13}\text{C}$  data, as well as Timothe Bolliet's database, will need to be added to the OC3 database in the future. Newer additions to the Pangaea database will also need to be copied into the OC3 database; the Cartapanis data collection featured all published NOAA and Pangaea data as of December 2011. Several datasets within the Schmittner collection were unable to be efficiently added at during the very beginning of database compilation and could be resolved to fit into the dataset with, for example, further correspondence with their author. These files should be added to OC3 if possible; their names and respective issues are detailed in the file "OC3 Database Notes: Andreas's Data Collection" in the Supplementary Materials folder. The newer NOAA sites are now included in OC3, but the Pangaea sites from the last few years are not. The OC3 database was created to be a living document and will only remain the most comprehensive  $\delta^{13}\text{C}$  database if newly published datasets are continually and faithfully added. Therefore, I expect that one important aspect of the database's future is publicizing its existence and soliciting new additions.

Beyond the scope of the Schmittner and Lund model, this database will prove highly valuable for future model/proxy comparisons by virtue of being the largest current collection of benthic  $\delta^{13}\text{C}$  information. Model-proxy comparison is an aspect of analysis of  $\delta^{13}\text{C}$  trends that did not fit within the scope of this project. A comparison of  $\delta^{13}\text{C}$  changes in data from the OC3 database with results from the model used in Schmittner and Lund 2015 would serve multiple useful purposes. It would allow for extrapolation beyond the spatial bounds of these datasets—as multiple latitudinal, longitudinal, and depth areas currently feature spotty data density—and, if the ages of the cores under scrutiny were well-constrained, could provide an opportunity to evaluate the

accuracy of the model using a wider range of observations than ever before. A recommended continuation of this analysis is to compare time series from one box of the model against a high-resolution, well-dated core located in the same area as the model box. Further refining of age information in the database will render the comparison of contour plots such as Figure 9 with modeled cross-sections of ocean basins such as Appendix 2 (Schmittner and Lund 2015) additionally feasible and useful. The utility of this large data collection in investigating deglacial circulation changes will be further improved as modeled starting conditions are refined.

The single largest and most important area for future work in this database is the addition, checking, and refinement of age models. The ideal state of the OC3 database would be to locate all  $\delta^{13}\text{C}$  information along a single, common, verified timescale. While this goal is not realistically achievable for 100% of sites in OC3 because of the variety of data sources, the database will be increasingly useful as more and better age models are matched with the sites. Working with the age information will come in many forms. As of now, many sites in the database do not have age information attached at all. In order to date these datasets, software developed by Lorraine Lisiecki, Match, could be used to align the  $\delta^{18}\text{O}$  information of the undated core with that of a core with a well-constrained age model. For this work, high-resolution cores should be prioritized. Another dating concern apparent at the closing of this project is the necessity for aligning currently-included age models. As is clearly and startlingly displayed in Figure 10, the  $\delta^{18}\text{O}$  of many cores from the same region show different patterns with different timing. The large disparity between  $\delta^{18}\text{O}$  curves likely indicates that these sites' age models are not harmonious, and software such as Match could be used to correct for this difficulty. One other area of improvement in OC3 sites' age models is the wide variety of temporal resolutions represented within the database's current contents, also shown in Figure 10. Match can likely be used to improve the resolution of age models that are currently sparse in dates. This software will be an important and potentially highly consistent method of ensuring that the age data in the OC3 database is as consistently present, high-resolution, and accurate as possible. Much of the noisiness of my analysis, as evidenced in Figure 10, Figure 11, and the time series and contour plots of  $\delta^{13}\text{C}$

change, could be reduced with verification and alignment of age models, making for a more definitive analysis.

### Acknowledgments

I would like to thank the National Science Foundation and Oregon State University's College of Earth, Ocean, and Atmospheric Sciences for providing the funding and facilities for this investigation, I am especially grateful to Kaplan Yalcin and Itchung Cheung, the directors of this REU program. I would like to thank my mentor, Andreas Schmittner, for his help and guidance throughout the course of this project. I am grateful for the enormous data contribution and technical support from Olivier Cartapanis, and for the contributions of age models by Lorraine Lisiecki and Carlye Peterson. I would like to thank Carrie Morrill from NOAA for her cooperation in identifying datasets for the project. Lastly, I would like to thank Dave Ullman and Drew Gleeman for their guidance in programming issues.

### Works Cited

- Duplessy, J. C., Shackleton, N. J., Matthews, R. K., Prell, W., Ruddiman, W. F., Caralp, M., & Hendy, C. H. (1984). 13 C record of benthic foraminifera in the last interglacial ocean: Implications for the carbon cycle and the global deep water circulation. *Quaternary Research*, 21(2), 225-243.
- Lisiecki, L.E., and P.A. Lisiecki, Application of dynamic programming to the correlation of paleoclimate records, *Paleoceanography*, 17(D4), 1049, doi:10.1029/2001PA000733, 2002.
- Liu, A. Z., He, F., Brady, E. C., Tomas, R., Clark, P. U., Carlson, A. E., ... Brady, E. C. (2009). Transient Simulation of Last Deglaciation with a New Mechanism for Bølling-Allerød Warming, 325(5938), 310–314.
- Lund, D. C., Tessin, a C., Hoffman, J. L., & Schmittner, a. (2015). Southwest Atlantic water mass evolution during the last deglaciation, (Figure 1), 1–18. <http://doi.org/10.1002/2014PA002657>.

- Lynch-Stieglitz, J., Adkins, J.F., Curry, W.B., Dokken, T., Hall, I.R.... Zahn, R. (2007). Atlantic Meridional Overturning Circulation During the Last Glacial Maximum. *Science*, 316(5821), 66-69.
- Marcott, S. A., Bauska, T. K., Buizert, C., Steig, E. J., Rosen, J. L., Cuffey, K. M., ... & Brook, E. J. (2014). Centennial-scale changes in the global carbon cycle during the last deglaciation. *Nature*, 514(7524), 616-619.
- McManus, J. F., Francois, R., Gherardi, J.-M., Keigwin, L. D., & Brown-Leger, S. (2004). Collapse and rapid resumption of Atlantic meridional circulation linked to deglacial climate changes. *Nature*, 428(6985), 834–837. <http://doi.org/10.1038/nature02494>
- Mignot, J., Ganopolski, A., & Levermann, A. (2007). Atlantic subsurface temperatures: Response to a shutdown of the overturning circulation and consequences for its recovery. *Journal of Climate*, 20(19), 4884–4898. <http://doi.org/10.1175/JCLI4280.1>
- Oppo, D. W., Curry, W. B., & Mcmanus, J. F. (2015). What do benthic  $^{13}\text{C}$  and  $^{18}\text{O}$  data tell us about Atlantic circulation during Heinrich Stadial 1?, 1–16. <http://doi.org/10.1002/2014PA002667>.Received
- Schmitt, J., Schneider, R., Elsig, J., Leuenberger, D., Lourantou, a., Chappellaz, J., ... Fischer, H. (2012). Carbon Isotope Constraints on the Deglacial  $\text{CO}_2$  Rise from Ice Cores. *Science*, 336(6082), 711–714. <http://doi.org/10.1126/science.1217161>
- Schmittner, A. (2005). Decline of the marine ecosystem caused by a reduction in the Atlantic overturning circulation. *Nature*, 434(7033), 628–633. <http://doi.org/10.1038/nature03476>
- Schmittner, A., & Galbraith, E. D. (2008). Glacial greenhouse-gas fluctuations controlled by ocean circulation changes. *Nature*, 456(7220), 373–376. <http://doi.org/10.1038/nature07531>

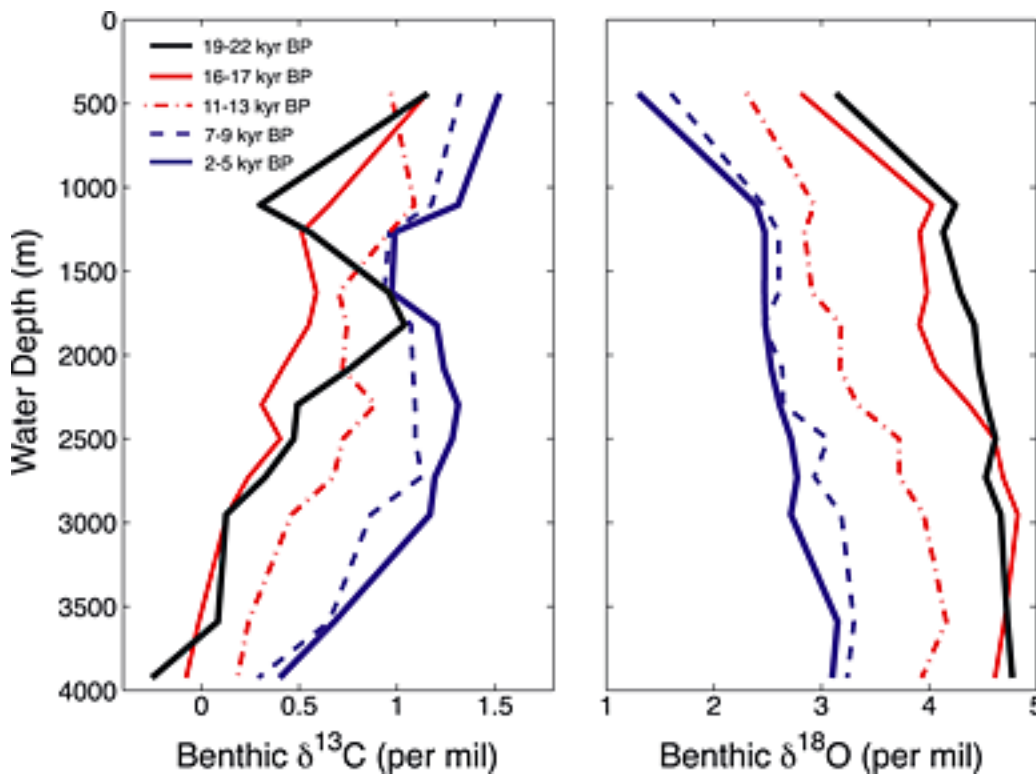
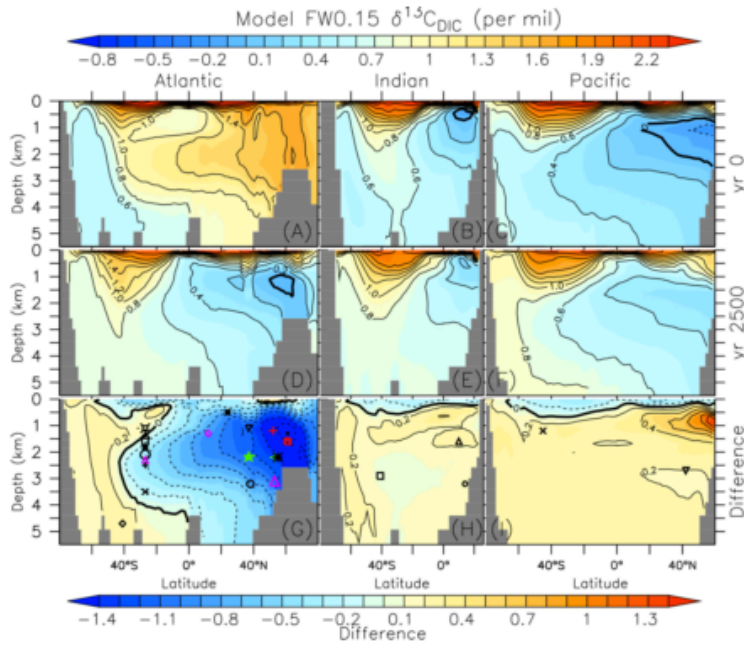
- Schmittner, A., & Lund, D. C. (2015). Early deglacial Atlantic overturning decline and its role in atmospheric CO<sub>2</sub> rise inferred from carbon isotopes ( $\delta^{13}\text{C}$ ). *Climate of the Past*, *11*(2), 135–152. <http://doi.org/10.5194/cp-11-135-2015>
- Schmittner, A., Gruber, N., Mix, A. C., Key, R. M., Tagliabue, A., & Westberry, T. K. (2013). Biology and air–sea gas exchange controls on the distribution of carbon isotope ratios ( $\delta^{13}\text{C}$ ) in the ocean. *Biogeosciences Discussions*, *10*(5), 8415–8466. <http://doi.org/10.5194/bgd-10-8415-2013>
- Stern, J. V., & Lisiecki, L. E. (2014). Termination 1 timing in radiocarbon-dated regional benthic  $\delta^{18}\text{O}$  stacks. *Paleoceanography*, *29*(12), 1127–1142.
- Thiagarajan, N., Subhas, A. V., Southon, J. R., Eiler, J. M., & Adkins, J. F. (2014). Abrupt pre-Bølling-Allerød warming and circulation changes in the deep ocean. *Nature*, *511*(7507), 75–8. <http://doi.org/10.1038/nature13472>

## Appendix A

List of supplementary materials included in Dropbox folder:

- OC3 Master Spreadsheet
- Google doc containing info on files from Schmittner database that should still be added to OC3 database
- Sites from Olivier Cartapanis' depthflagged database that have depth and carbon information (my research partner, Aaron Rachels, put the entirety of the Cartapanis database in the Valis Scratch drive)
- Spreadsheets generated by Cartapanis code: relevant data from initial database (of depthflagged sites) and database for entire Cartapanis collection (incl. non-depthflagged)
- Cartapanis Matlab script for extraction of data from Matlab database
- Spreadsheets of Stern and Lisiecki age models provided by Carlye Peterson
- Map of sites updated with Stern and Lisiecki age models
- My Google Doc of progress throughout the summer
- ReadMe file with more detailed description and instruction for Supplementary Materials items
- Code in R used to perform data analyses
- Various figures
- .csv files of millennial and period averages, as well as millennial and whole deglacial standard deviation, and regression models for each millennium of each region.

Appendix  
 2. Modeling results of  $\delta^{13}C$  changes as a response to an AMOC shutdown in different ocean basins from Schmittner and Lund 2015. Top: active AMOC, center: shutdown AMOC, bottom: difference.



Appendix 3. Lund et al. 2015: vertical profiles of  $\delta^{13}C$  (left) and  $\delta^{18}O$  (right) from Brazil Margin cores.

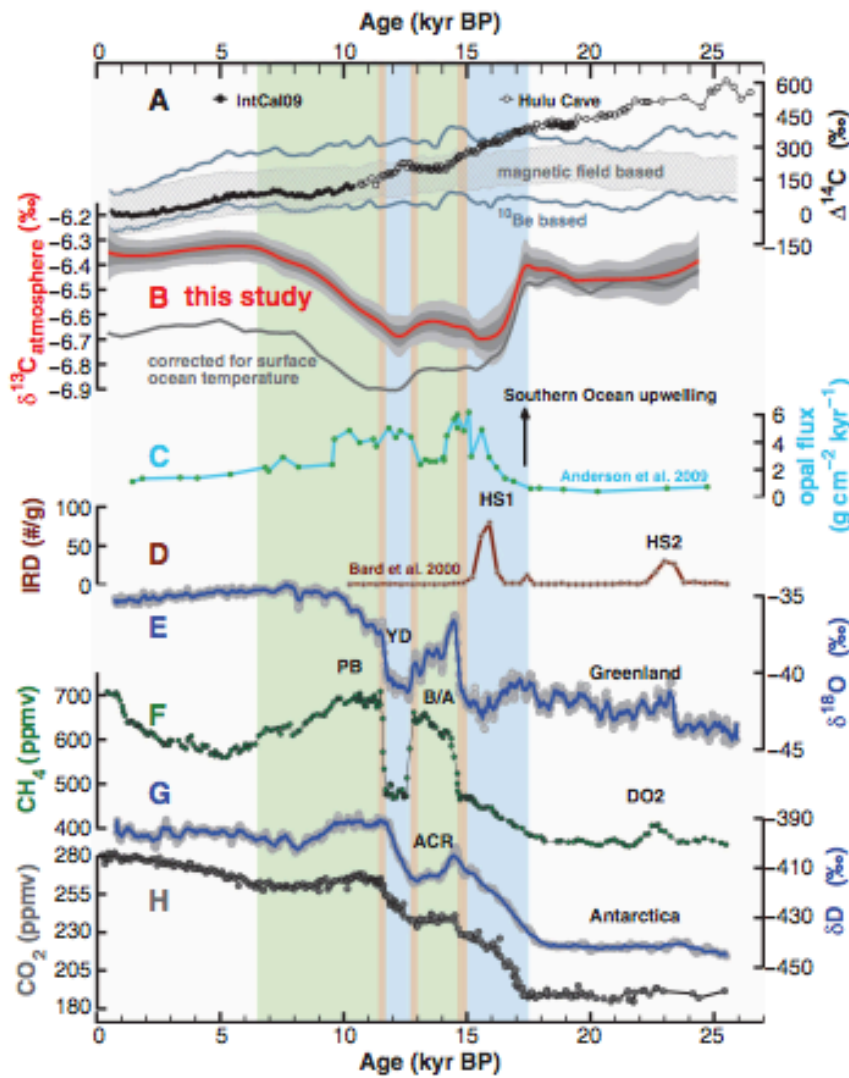
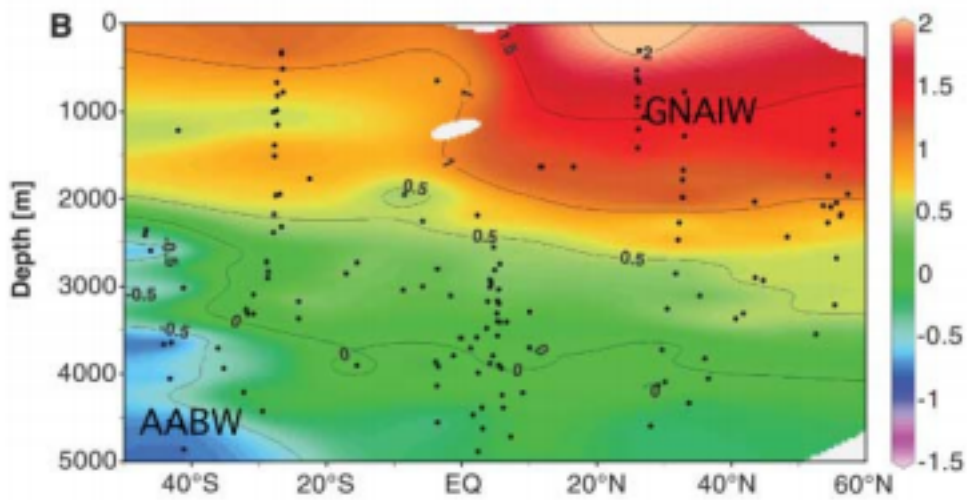
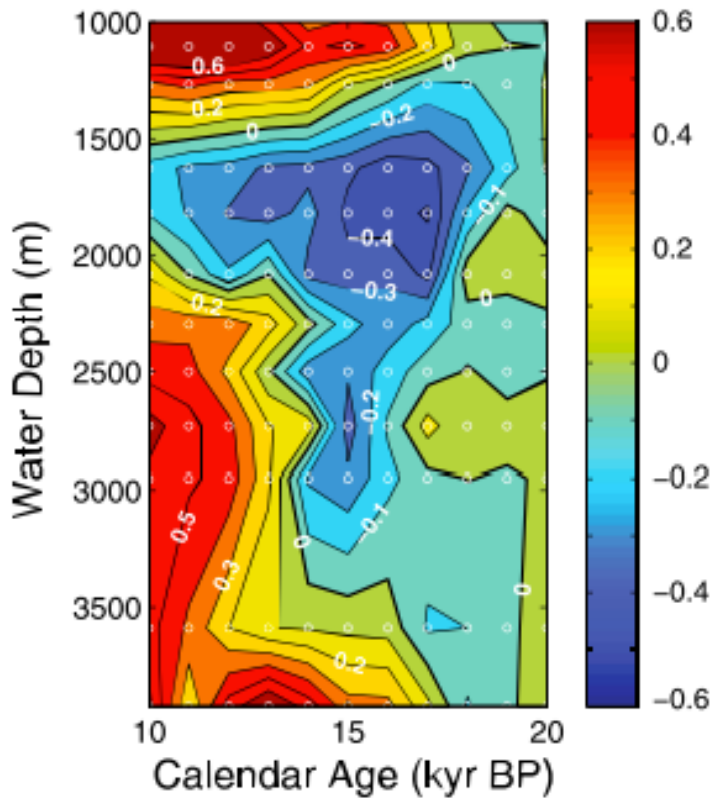


**Fig. 2.** Ice core reconstructions and marine records illustrating the evolution of major components of the Earth climate system over the past 24,000 years. (A) Reconstructed  $\Delta^{14}\text{C}_{\text{atm}}$  from IntCal09 (14) and the  $^{230}\text{Th}$ -dated Hulu Cave  $\Delta^{14}\text{C}_{\text{atm}}$  record (15) compared with modeled (16)  $\Delta^{14}\text{C}_{\text{atm}}$  assuming a constant carbon cycle under preindustrial conditions but considering temporal changes in  $^{14}\text{C}$  production [based on  $^{10}\text{Be}$  (18), upper and lower estimates (gray lines), or based on paleomagnetic field intensity (17), hatched area]. (B) Monte Carlo average (this study) of the evolution of  $\delta^{13}\text{C}_{\text{atm}}$  before SST correction (red line represents the MCA;  $2\sigma$  and  $1\sigma$  envelopes are in gray) and after SST correction (gray line). (C) Opal flux in the Southern Ocean as a proxy for local upwelling (20). (D) Record of ice-rafted debris (IRD) in the North Atlantic associated with Heinrich stadials HS1 and HS2 (27). (E) Greenland temperature proxy  $\delta^{18}\text{O}$  (33). (F) Reconstructed atmospheric  $\text{CH}_4$  concentration (34). (G) Antarctic temperature proxy  $\delta\text{D}$  from the EDC ice core (35). (H) Compilation of reconstructed  $\text{CO}_2$  shown in Fig. 1B. Green bars indicate intervals with a strong net terrestrial carbon buildup; blue bars indicate intervals where sequestered deep ocean  $\text{CO}_2$  was released back to the atmosphere. Note that ice core records are plotted on a synchronized age scale (32), whereas other records are plotted on their individual age scales. PB, Preboreal; YD, Younger Dryas; B/A, Bølling-Allerød warming; DO2, Dansgaard-Oeschger event 2; ACR, Antarctic Cold Reversal.

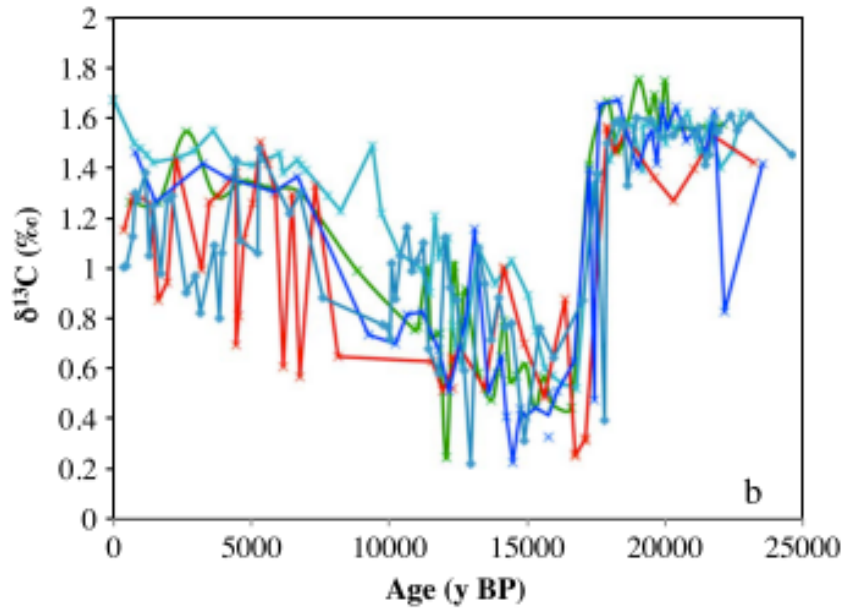
Appendix 4. Schmitt et al. 2012.



Appendix 5. Lynch-Stieglitz et al. 2007; the Last Glacial Maximum distribution of  $\delta^{13}\text{C}$  of benthic foraminifera in western and central Atlantic.



Appendix 6. Lund et al. 2015; benthic  $\delta^{13}\text{C}$  anomaly for the last deglacial period, showing showing  $\delta^{13}\text{C}$  value minus mean LGM value at that depth.



Appendix 7. Oppo et al., 2015; benthic  $\delta^{13}\text{C}$  for ODP984, NEAP4k, and EW9302 cores versus age.